

Confinement and transverse conductivity in coupled Luttinger liquids

S. Capponi, D. Poilblanc and F. Mila
*Laboratoire de Physique Quantique,
Université Paul Sabatier, 31062 Toulouse, France.*
(June 96)

One-particle interchain hopping in a system of coupled Luttinger liquids is investigated by use of exact diagonalizations techniques. Firstly, the two chains problem of spinless fermions is studied in order to see the behaviour of the band splitting as a function of the exponent α which characterizes the 1D Luttinger liquid. Moderate intra-chain interactions can lead to a strong reduction of this splitting. The on-set of the confinement within the individual chains (defined by a vanishing splitting) seems to be governed by α . We give numerical evidence that inter-chain coherent hopping can be totally suppressed for $\alpha \sim 0.4$ or even smaller α values. The transverse conductivity is shown to exhibit a strong incoherent part. Even when coherent inter-chain hopping is believed to occur (at small α values), it is shown that the coherent Drude weight is always significantly smaller than the incoherent weight. Implications for the optical experiments in quasi-1D organic or high- T_c superconductors is outlined.

PACS numbers: 74.72.-h, 71.27.+a

Recently, the study of strongly correlated fermions confined to coupled chains has received a great deal of interest in particular as a way of studying the dimensional cross-over from 1D Luttinger-like behaviour to 2D.

Some time ago, Anderson emphasized the crucial difference between in-plane and inter-plane (c-axis) transport observed in copper oxide superconductors [1]. Indeed, experimentally the c-axis transport has an anomalous behaviour [2] in the sense that the transverse conductivity has a completely incoherent frequency dependence, there seems to be no sizeable Drude-like term (except in the optimally doped systems) and $\sigma(\omega)$ is a very slowly increasing function of the frequency. This phenomenon has been interpreted as an incoherent hopping or as the “confinement” of the electrons inside the weakly coupled planes. However, for coupled Fermi liquids (FL), Landau theory predicts coherent transverse hopping and no anomalous transport. Therefore, it has been suggested that anomalous transport in the direction of low conductivity is precisely the signature that the ground state (GS) of the two-dimensional (2D) plane itself is not of the usual FL type. Various candidates for this state have been proposed, such as the marginal Fermi liquid [3] or the Luttinger liquid (LL) which is generic in one dimension (1D) [4].

Although non-Fermi liquid (NFL) behaviour is thought to occur in the planes of high temperature superconductors (HTSC), it has been impossible yet to prove the NFL nature in 2D except for unrealistic models. However, as stated above, it is well known that the generic features of correlated 1D electrons are not FL-like but rather those of a LL and the precise nature (asymptotic behaviour, exponents, etc...) of the system can be easily controlled. In addition, quasi-1D systems are realized in nature, and

the problem of coupled chains is of direct relevance there. For instance, in the case of the organic superconductors of the $(\text{TMTSF})_2\text{X}$ family [5], also known as the Bechgaard salts, the high temperature properties are believed to be essentially one-dimensional, while the low-temperature behaviour is three-dimensional. This cross-over is presumably responsible for the anomalies observed in the temperature dependence of several quantities (such as the $2k_F$ contribution to the relaxation rate [6], the ratio of the perpendicular conductivity to the parallel one [5], the plasma edge when the electric field is polarized perpendicular to the chains [5],...) as well as for the insulating behaviour reported for $(\text{TMTSF})_2\text{ClO}_4$ in the presence of a strong enough magnetic field [7]. Although a lot of work has already been devoted to that problem [7,8], several aspects of this cross-over have to be better understood, in particular those concerned with the transport properties perpendicular to the chains.

Hence, from now on and for sake of simplicity, we shall only deal with weakly coupled chains.

The effect of single-particle transverse hopping has previously been studied from a renormalization group point of view [8]. The notions of interchain coherence or incoherence have emerged from such an analysis. Let us recall here that a LL has a different structure from FL: there are no quasi-particle like excitations but instead collective modes (charge and spin) with different velocities which lead to the so-called spin-charge separation; moreover, the density of states $n(k)$ has no step-like structure at the Fermi level but instead a power law singularity $n(k) - n(k_F) \sim |k - k_F|^\alpha$ defining the parameter α which depends on the intra-chain interaction. It turns out that the hopping t_\perp is a relevant perturbation when $\alpha \leq 1$ [8].

However, it has been argued that relevance in that

sense was not necessarily a sufficient condition to cause coherent motion between chains. This, e.g., can be seen from the following model [9]; let a system of two separated chains be prepared at time $t = 0$ with a difference of ΔN particles between the two chains. Then, the interchain hopping is turned on and one considers the probability of the system of remaining in its initial state, $P(t)$. Coherence or incoherence can then be defined as the presence or absence of oscillations in $P(t)$.

In Ref. [9], the authors restricted themselves to the short time behaviour of $P(t)$ which, they argued, can provide valuable informations on interchain coherence or incoherence. They found two regimes which depend entirely on the value of α : the case $\alpha < 1/2$ exhibited coherent motion while $\alpha > 1/2$ showed no signal of coherence. However, as has been shown numerically and argued in Ref. [11], the small time behaviour can not always distinguish between coherent or incoherent regimes. In addition, if the initial state is far from equilibrium, i.e. if $\Delta N/N$ is not infinitesimal, then mathematical properties of the many-body spectrum related to the integrability or non integrability of the model will play a central role. Indeed, in this case, coherent behaviour is found [11] to be a generic property of integrable models (irrespective of the value of α). However, it is not clear whether this conclusion remains for low energy excitations.

Another possible issue which has been raised is whether the spin degrees of freedom are essential in Anderson's confinement mechanism or not [10]. The two chain problem with no anomalous exponent ($\alpha = 0$) but with spin-charge separation features was solved exactly in [12] and showed no confinement within each chain i.e. an energy separation was found between the bonding and anti-bonding states. This result *a priori* does not contradict Anderson's conjecture which claims that the behaviour only depends on α . However, it is still not clear whether confinement can be found for spinless models with large α 's and whether the fact that the low energy excitations of the spinless fermion chain are collective modes is sufficient to, alone, produce confinement in the chains.

This paper is devoted to the study of various aspects of interchain coherence in systems of strongly correlated spinless fermions. We shall derive several quantities sensitive to the coherent/incoherent nature of the hopping transverse to the chains from exact diagonalizations of small systems by the Lanczos algorithm [13]. After a short presentation of the models in Sec. I, a precise characterization of the single chain system in terms of its LL parameters is given in Sec. II for models with screened interactions extending in space up to third neighbours. In Sec. III, we study the simplest case of two coupled chains. The influence of the interchain hopping on the splitting in energy of the singularities appearing in the spectral function for $k_{\perp} = 0$ and π is studied, in a similar way as has been done for particles with spin [14]. Using different models with different extensions in space of the interaction, we investigate whether the physics de-

pends only on the LL parameter α or not. In order to establish possible connections between the splitting and transport properties, we consider in Sec. IV a system of three coupled chains. Periodic boundary conditions in the transverse direction are used in order to derive the optical conductivity in this direction, hence, providing a direct (and experimentally observable) test of the confinement of the fermions within the chains.

I. THE MODEL

We consider here a model of spinless fermions on a lattice formed by m chains of length L with a weak interchain hopping:

$$H = - \sum_{j,\beta} (c_{j+1,\beta}^{\dagger} c_{j,\beta} + \text{H.c.}) - t_{\perp} \sum_{j,\beta} (c_{j,\beta+1}^{\dagger} c_{j,\beta} + \text{H.c.}) + \sum_{j,\beta,\delta} V(\delta) n_{j,\beta} n_{j+\delta,\beta} \quad (1)$$

where β labels the chain ($\beta = 1, \dots, m$), j is a rung index ($j = 1, \dots, L$), $c_{j,\beta}$ is the fermionic operator which destroys one fermion at site j on the chain β , and $V(\delta)$ is a repulsive interaction between two fermions at a distance δ (the lattice spacing has been set to one). For convenience, we choose a repulsive interaction of the form $V(i) = 2V/(i+1)$ for $i \leq i_0$, with, more specifically, $i_0 = 1, 2, 3$ which corresponds to an interaction extending up to first, second and third nearest neighbours (NN) respectively.

In the x and y-directions, we shall use arbitrary boundary conditions (BC) by threading the system with a magnetic flux Φ_x and Φ_y respectively (except for $m = 1$ or 2 chains where open BC are used in the y-direction). This is realized by a Peierls substitution that modifies the kinetic term, e.g. a twist along the transverse direction is realized by

$$c_{j,\beta+1}^{\dagger} c_{j,\beta} \rightarrow c_{j,\beta+1}^{\dagger} c_{j,\beta} e^{i \frac{2\pi}{m} \Phi_y} \quad (2)$$

where Φ_y is the flux measured in unit of the flux quantum $\Phi_0 = hc/e$. Similarly, the hopping term in the x-direction contains a phase $\frac{2\pi}{L} \Phi_x$.

The motivation to introduce flux is two-fold. Firstly, as proposed by Kohn [15] transport properties of a correlated system can be directly measured from the response of the system to a twist in the boundary condition. Secondly, our ultimate goal is to extract quantities in the thermodynamic limit from finite size scaling analysis. It turns out that a simple way to improve the accuracy for a fixed system size is to average over the boundary conditions e.g. over Φ_y and/or Φ_x [16,17].

II. LL PARAMETERS FOR THE SINGLE CHAIN

In order to characterize the behaviour of coupled chains, it is required to, first, compute the parameters of a single chain for the same model. Indeed, one important issue is to study whether interchain transport is a universal function of the LL parameters or whether it depends on the details of the model. In the case of NN interactions, the hamiltonian (known as the t-V model) can be mapped onto a spin chain problem by a Jordan-Wigner transformation and this is exactly soluble by the Bethe ansatz; thus, α is known for each filling [4]. However, for extended interactions in space, a numerical investigation is necessary with the help of conformal invariance identities. It turns out that the exponent α can be related to simple physical quantities which can be easily extracted from standard exact diagonalization results using the Lanczos algorithm. For instance the Drude weight $2\pi D$ (D is the charge stiffness) and the charge velocity u_ρ are related by [18]

$$2\pi D = 2u_\rho K_\rho, \quad (3)$$

where K_ρ is a universal parameter which determines the long distance behaviour of the correlation functions. The quantities u_ρ and D can be directly obtained on finite systems. The Drude weight for a single chain is given by the Kohn formula:

$$2\pi D = \frac{1}{4\pi} \frac{\partial^2(E_0/L)}{\partial \Phi_x^2} \quad (4)$$

The charge velocity can be extracted from the difference in energy of the two singlet symmetry sectors $k = 0$ and $k = 2\pi/L$ (for an even number of fermions). K_ρ is then obtained from Eq. (3) and the density of state exponent (for spinless fermions) can be calculated as [18]

$$\alpha = \frac{1}{2} \left(K_\rho + \frac{1}{K_\rho} - 2 \right) \quad (5)$$

Finite size scaling analysis reveals that the $1/L^2$ law for the finite size corrections is very well satisfied for K_ρ and α so that an accurate determination of the extrapolated values can be calculated. Results for α are plotted in Fig. 1.

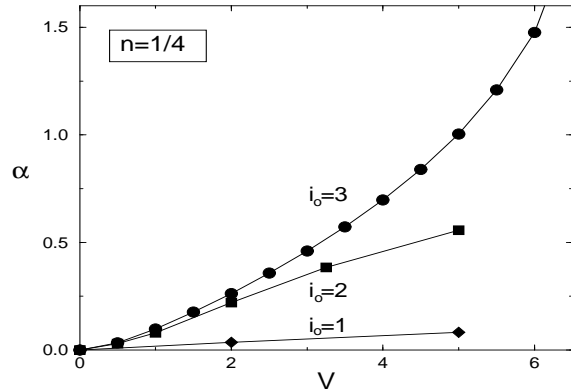


FIG. 1. Exponent α vs V for $n = 1/4$ and for NN interaction (\blacklozenge) and longer range $i_0 = 2$ (\blacksquare), $i_0 = 3$ (\bullet).

As is expected, the value of α increases with the strength of the interaction and with its range in space. However, for a given filling, there is a maximum allowed value α_{max} for α [20]. Above this value, Umklapp processes become relevant, a gap opens up in the single particle spectrum and the system undergoes a metal-insulator transition. The insulating phase is signalled by both an opening of the single particle gap and by a vanishing Drude weight [15]. This region is of no interest to us in the present study since no transverse hopping occurs when t_\perp is smaller than the single particle gap. For a given density, α acquires its maximum value on the metal-insulator transition line. It is important to notice that this maximum value depends only on the density and, hence, the commensurability: if $n = p/q$, it is larger for larger q . As an example, for $n = 1/2$ $\alpha_{max} = 1/4$ while for $n = 1/4$ a value as large as $\alpha_{max} = 49/16 \simeq 3.06$ can be obtained. This fact has motivated our choice of $n = 1/4$ for the following calculations since it gives a large range of α values. Typically, for $n = 1/4$, α_{max} is realized by $i_0 = 3$ and $V \simeq 7.5$. For a shorter range interaction, significantly larger values of V are necessary.

III. INTERCHAIN COHERENCE

The simplest approach to investigate interchain coherence is to consider 2 coupled chains, i.e. a $2 \times L$ ladder. We proceed along the lines of Ref. [14]. In the absence of interaction, t_\perp leads to bonding and anti-bonding dispersion bands corresponding to transverse momentum $k_\perp = 0$ or π respectively, as seen in figure 2. The splitting $2t_\perp$ between these bands can be viewed as the signature of a coherent transverse hopping. These bands correspond to a δ -function singularity in the single particle hole (electron) spectral function for $k < k_F$ ($k > k_F$). The hole spectral function is defined by,

$$A_h(\mathbf{k}, \omega) = -\frac{1}{\pi} \text{Im} \left\{ \langle \phi_0 | c_{\mathbf{k}}^\dagger \frac{1}{\omega + i\varepsilon - H + E_0} c_{\mathbf{k}} | \phi_0 \rangle \right\} \quad (6)$$

where $\mathbf{k} = (k, k_\perp)$ and a similar definition holds for A_e by exchanging $c_{\mathbf{k}}^\dagger$ and $c_{\mathbf{k}}$.

In the case of interacting particles, this δ -function singularity is replaced by a power law singularity and the elementary excitations are collective modes. Here, we address the issue of the influence of the hopping t_\perp on this singularity, in particular we investigate whether a splitting occurs. The choice of the boundary conditions in the x-direction is expected to be important in the scaling behaviour of various quantities. Periodic or anti-periodic BC lead to closed or open shells as can be seen in figure 2. We shall consider these two cases separately.

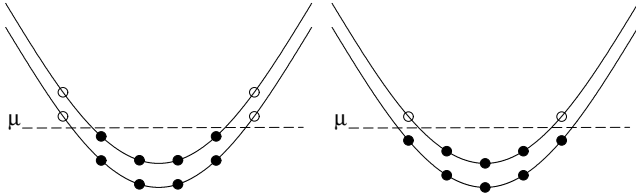


FIG. 2. Dispersion relation along the chain direction in the closed (left) and open (right) shell configurations. Full (open) symbols correspond to occupied (empty) states and μ is the chemical potential.

A. Splitting: closed shell configuration

In the closed shell configuration of Fig. (2), we can add (respectively remove) one fermion on either of the two branches (characterized by the transverse momentum k_\perp) just above (resp. below) the FL and then calculate the GS energy of this new system. The difference between the two values of the energy gives the splitting ΔE between the two bands.

For interacting particles, ΔE can be alternatively (and more precisely) defined as the energy separation between the two low energy peaks in the spectral function $A_h(\mathbf{k}, \omega)$ and $A_e(\mathbf{k}, \omega)$ for $k_\perp = 0$ and $k_\perp = \pi$. For a longitudinal momentum k chosen above or below the (non-interacting) Fermi wavevector $k_F = \pi n$ the electron (hole) spectral function has to be considered. We have performed exact diagonalizations on clusters $2 \times 4p$ with $p = 1, \dots, 5$ at $n = 1/4$ to obtain the splitting for different values of the parameters. Results for a 2×16 ladder at $n=1/4$ are shown in Fig. (3) (a) and (b) for two momenta $k < k_F$ and $k > k_F$. The results look similar to the non-interacting case although the splitting between the $k_\perp = 0$ and $k_\perp = \pi$ structures is reduced. Let us remark that a new structure appears for $\omega < \mu$ and $k > k_F$. It is completely absent in the non-interacting case but was predicted by Voit [19] for large α 's by using a low energy bosonization scheme. Note, however, that such

calculations can not resolve the fine structure of the LL singularity.

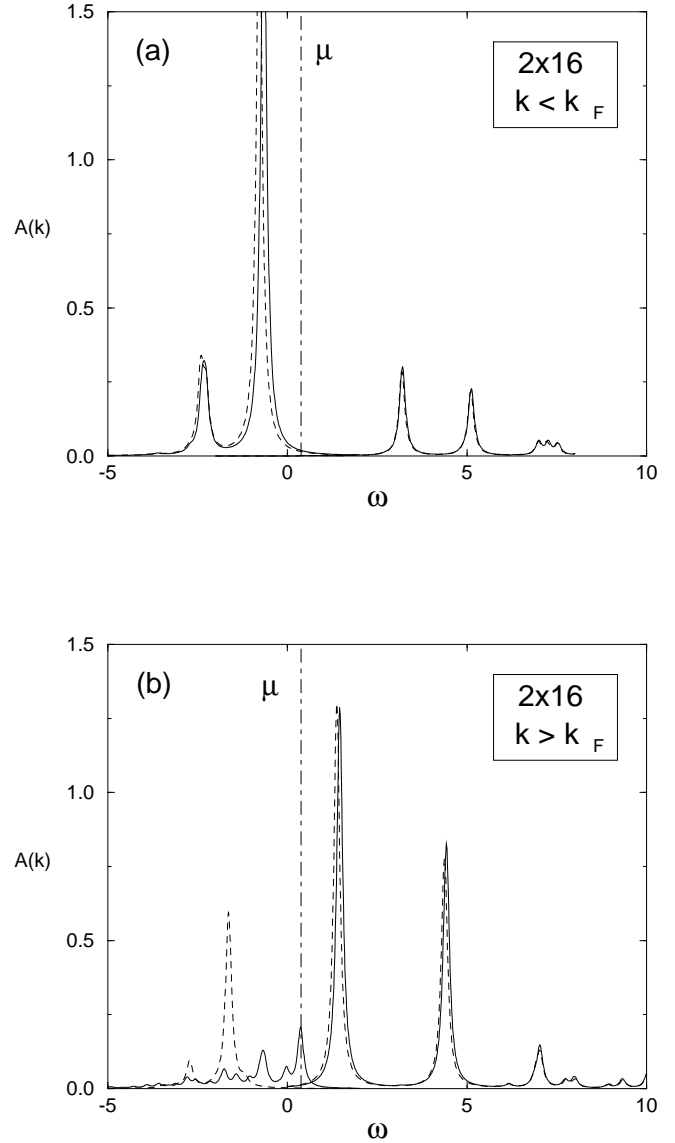


FIG. 3. Spectral function vs ω for the case $V = 5$, $i_0 = 2$ with $t_\perp = 0.1$. The regions $\omega < \mu$ and $\omega > \mu$ correspond to $A_h(\mathbf{k}, \omega)$ and $A_e(\mathbf{k}, \omega)$ respectively. The full (dotted) lines correspond to $k_\perp = \pi$ ($k_\perp = 0$). (a) (resp. (b)) corresponds to a momentum below (resp. above) k_F . An artificial width ε has been added to the frequency, $\omega \rightarrow \omega + i\varepsilon$.

A careful study of the exact diagonalizations data reveals that ΔE , for small t_\perp , behaves like $at_\perp + bt_\perp^3$ and the coefficient a can be calculated accurately. Finite size corrections of the order of $1/L$ have been found for a so that $\lim_{t_\perp \rightarrow 0} \Delta E / 2t_\perp$ can be estimated accurately in the thermodynamic limit. In Fig. 4, we plot, as a function of α , the average between the splittings above and below the FL as well as the extrapolated value. The (normalized) splitting is greatly reduced by the electronic inter-

actions (measured by α) but it does not seem to vanish for $\alpha = 0.5$. On the contrary, it is compatible with the RG approach predicting that t_{\perp} becomes irrelevant, and hence that $\lim_{t_{\perp} \rightarrow 0} \Delta E/2t_{\perp}$ vanishes, only for $\alpha > 1$.

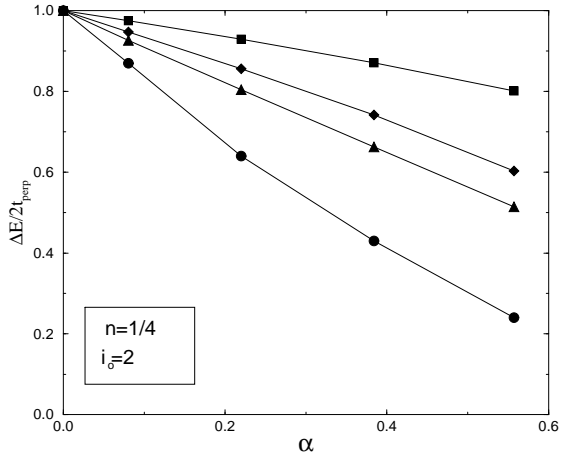


FIG. 4. $\lim_{t_{\perp} \rightarrow 0} \Delta E/2t_{\perp}$ ($=a$) vs α for various system sizes and extrapolated values. Closed shell configurations have been considered. An average between the splitting above and below k_F is performed. $L = 8$, $L = 12$ and $L = 16$ correspond to \blacksquare , \blacklozenge , \blacktriangle respectively.

However, these results must be considered with care for two reasons. First, it is clear that ΔE alone does not completely characterize the transverse hopping dynamics. As seen in Ref. [14], the return probability $P(t)$, for example, depends on the whole frequency dependence of $A_h(\mathbf{k}, \omega)$ (or $A_e(\mathbf{k}, \omega)$). Since, for large interactions, spectral weight from the LL singularity is transferred to higher excitation energies, then an incoherent behaviour of $P(t)$ can be found even though ΔE remains finite. Secondly, it should be stressed that the limit $t_{\perp} \rightarrow 0$ has been taken first before eventually taking the limit $L \rightarrow \infty$. Indeed, the linear behavior of the splitting with t_{\perp} is only valid in a narrow region which shrinks to zero as $1/L$. In other words, when $t_{\perp} \sim \pi v_{\rho}/L$ (v_{ρ} is some characteristic charge velocity), in the closed shell configuration, the excitation energy at $k_{\perp} = \pi$ for a longitudinal momentum just below k_F crosses the chemical potential so that the splitting cannot any longer be defined as some energy difference between many-body states corresponding to the same number of particles. To avoid such complications, we now consider the open shell configuration of Fig. (2).

B. Splitting: open shell configuration

As can be seen in Fig. (2), in the open shell configuration, one can add or remove a particle exactly at

the Fermi momentum which is independent of the system size. We thus define the splitting as the difference between the electron and hole excitation energies i.e. $E_0(N_e + 1, \mathbf{k}_e) - E_0(N_e)$ and $E_0(N_e) - E_0(N_e - 1, \mathbf{k}_h)$ where $E_0(N_e)$ is the reference energy corresponding to the absolute GS of the $N_e = nN$ electron system. The momenta for the electron and hole excitations are fixed, $\mathbf{k}_e = (k_F, \pi)$ and $\mathbf{k}_h = (k_F, 0)$. Note that, for a fixed value of t_{\perp} , these elementary excitations are not the lowest energy excitations in the thermodynamic limit (if t_{\perp} is relevant) since they have a longitudinal momentum k_F which is defined with respect to the single chain case (i.e. for $t_{\perp} = 0$). We then naturally define,

$$\Delta E = E_0(N_e + 1, \mathbf{k}_e) + E_0(N_e - 1, \mathbf{k}_h) - 2E_0(N_e). \quad (7)$$

For $V=0$, this expression exactly gives the splitting $2t_{\perp}$ for any system size. For $t_{\perp} = 0$ but finite interaction strength, ΔE is finite. However, Fig. (5) reveals that it scales to zero in the thermodynamic limit as expected. Fig. (5) also shows that an accurate finite size scaling analysis can be performed for finite interaction strength and finite t_{\perp} , assuming $1/L$ finite size corrections.

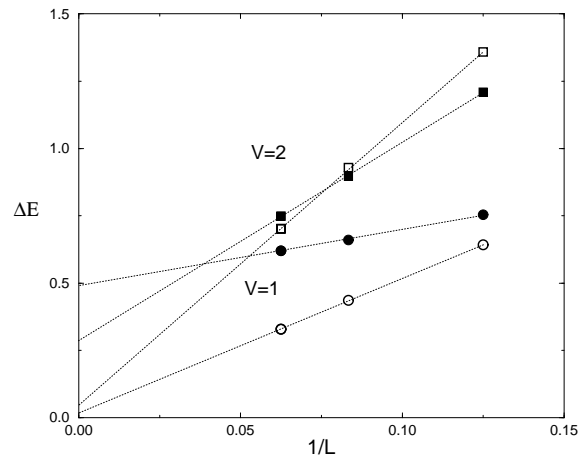


FIG. 5. ΔE vs $1/L$ for $t_{\perp} = 0$ (open symbols) and $t_{\perp} = 0.3$ (solid symbols). Interactions up to next nearest neighbors ($i_0 = 2$) with different strength V have been considered.

The extrapolated values ($L = \infty$) of the ratio $\Delta/2t_{\perp}$ are plotted as a function of the exponent α of the $i_0 = 2$ model (i.e. with interactions extending up to second nearest neighbors) in Fig. (6) for fixed interchain hopping amplitudes t_{\perp} . A strong reduction of this ratio for increasing α indicates that intrachain repulsion has a drastic influence in prohibiting interchain coherent hopping. Our data suggest that there is a critical value $\alpha^*(t_{\perp})$ such that interchain hopping becomes incoherent for $\alpha > \alpha^*(t_{\perp})$. As expected, $\alpha^*(t_{\perp})$ increases with t_{\perp} . Even for finite (but small) t_{\perp} , $\alpha^*(t_{\perp})$ can be as small as

0.4. The limiting value $\alpha^*(t_\perp = 0) = \alpha_0$, although not accurately given by our method, is probably significantly smaller than 0.4. This is indeed clear from Fig. (7) where the same ratio $\Delta/2t_\perp$ is plotted as a function of t_\perp for various interactions ($i_0 = 2$ model). For large interactions like $V = 3.25$ ($\alpha \sim 0.38$), there is a critical value $t_\perp^*(\alpha)$ of t_\perp below which incoherent transverse hopping takes place. This corresponds to the case $\alpha > \alpha_0$. For smaller interaction like $V = 1$ ($\alpha \sim 0.08$) our data are consistent with $\Delta/2t_\perp$ approaching a finite value when $t_\perp \rightarrow 0$. Hence, transverse hopping remains coherent in this case which corresponds to $\alpha < \alpha_0$. For intermediate interactions like $V = 2$ ($\alpha \sim 0.22$), our data are not conclusive. However, very small values of α_0 like 0.2 (or even smaller) are not inconsistent with our numerical analysis.

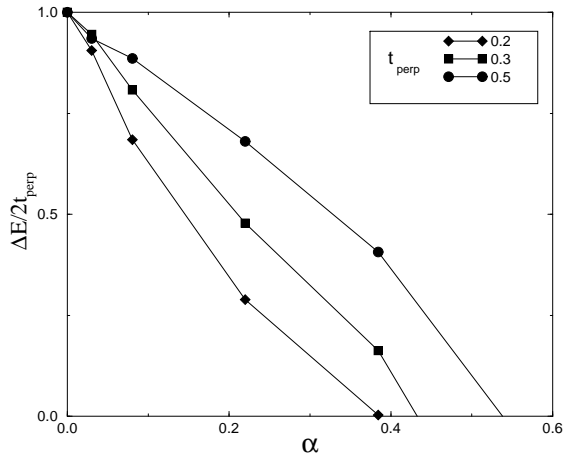


FIG. 6. Extrapolated ($L = \infty$) values of $\Delta E/2t_\perp$ vs α for several values of t_\perp (indicated on the figure) and in the $i_0 = 2$ spinless fermion model.

It is important to notice that the previous extrapolations carried out for open shell configurations and finite t_\perp give very different results than those shown in Fig. (4). In particular, Fig. (6) suggests that the critical value α_0 is significantly smaller than the value of 1 predicted by the RG analysis. One possible explanation is that the limits $t_\perp \rightarrow 0$ and $L \rightarrow \infty$ do not commute with each other. This scenario is supported by the fact that, in the closed shell configuration, the linear dependence of the splitting ΔE with t_\perp is limited, for increasing system size, to a narrower and narrower range of order $1/L$. Therefore, an extrapolation at finite t_\perp has to be realized. It is interesting to note that the RG approach seems, on the contrary, to reproduce the $\lim_{L \rightarrow \infty} \{ \lim_{t_\perp \rightarrow 0} (\Delta E/2t_\perp) \}$ data.

We shall finish this section with a brief comment on the role of the spin degrees of freedom which have not been considered here. It is clear that, when spin is taken

into account, the spin-charge separation that occurs in 1D should suppress even further the coherent transverse hopping. At a qualitative level, this can be understood from the fact that only real electrons can hop from one chain to the next and this is believed to become more difficult in the presence of spin-charge separation as has been suggested by Anderson [1]. Although dealing with a different filling $n = 1/3$ and with particles with spin, the same qualitative behaviour is found numerically in Ref. [14]; however, the decrease of the splitting with α is stronger.

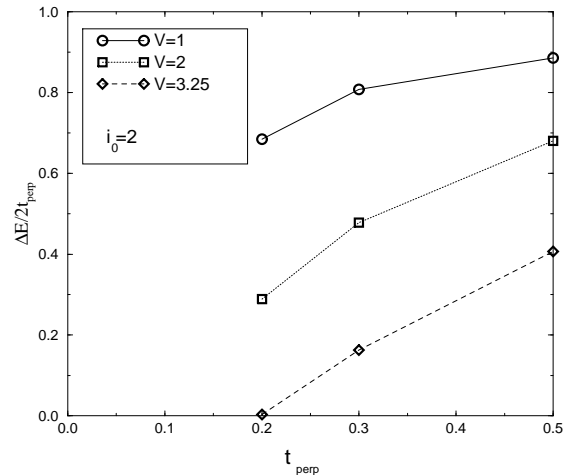


FIG. 7. Extrapolated ($L = \infty$) values of $\Delta E/2t_\perp$ vs t_\perp in the $i_0 = 2$ spinless fermion model with several values of V (indicated on the figure).

IV. TRANSPORT PROPERTIES

The previous study suggests that the interaction tends to confine the electrons within the chains, although no complete confinement seems to occur at small α values where $\Delta E \neq 0$. A better understanding of this phenomenon can be achieved by investigating the transport properties along the y-axis (inter chain) and more precisely the transverse optical conductivity which is the linear response of the system to a spatially uniform, time dependent electric field in the transverse direction. For such a study, a torus geometry is needed ($m \geq 3$) so that a current can flow around the loop in the y-direction. One of the main advantage of the optical conductivity is that it can directly be measured experimentally.

The real part of the optical conductivity can be written as a sum of two parts,

$$\sigma_{yy}(\omega) = 2\pi D_{yy} \delta(\omega) + \sigma_{yy}^{reg}(\omega) \quad (8)$$

where D_{yy} is the charge stiffness in the y-direction which defines the Drude weight $2\pi D_{yy}$. Note that an important f-sum rule [21] can be used to check the numerical results,

$$\begin{aligned}
\int_0^\infty d\omega \sigma_{yy}(\omega) &= \frac{\pi e^2}{2N} \langle t_\perp \sum_{j,\beta} (c_{j,\beta+1}^\dagger c_{j,\beta} + \text{H.c.}) \rangle \\
&= -\frac{\pi e^2}{2N} T_{yy},
\end{aligned} \tag{9}$$

where the expression between brackets is the mean value of the transverse kinetic energy in the ground state.

The actual calculation of the frequency dependence of $\sigma_{yy}^{reg}(\omega)$ will be carried out later on and we first concentrate on D_{yy} and on the total sum rule. As originally noted by Kohn [15], D_{yy} , which measures a transport quantity, can be obtained from the dependence of the ground state energy E_0 on Φ_y as

$$2\pi D_{yy}(\Phi_y) = \frac{m^2}{4\pi} \frac{\partial^2 (E_0/N)}{\partial \Phi_y^2} \tag{10}$$

where $N = mL$ is the number of sites. This is, in all points, very similar to the previous derivation of the charge stiffness D for the 1D rings.

The previous quantities have been calculated numerically on finite $3 \times L$ lattices using the Lanczos algorithm. We have chosen a quarter filled band so that the extrapolation of results for $L = 4, 8$ and 12 is possible. From now on, we shall restrict ourselves to PBC or ABC in the x-direction. In most cases, an average over Φ_y is realized [16,17] in order to mimic the case of many parallel chains i.e. we calculate,

$$\langle D_{yy} \rangle_{\Phi_y} = \int_{-1/2}^{1/2} d\Phi_y D_{yy}(\Phi_y). \tag{11}$$

This is done by calculating the ground state energy for a (large) discrete set of flux values (still making use of the translational invariance). A typical curve for $E_0(\Phi_y)$ is shown in Fig. (8) and reveals that level crossings occur as a function of Φ_y . As for the ladder case, the scaling behaviour depends crucially on the choice of the boundary conditions along the x-direction. In the following, we shall study two different cases separately.

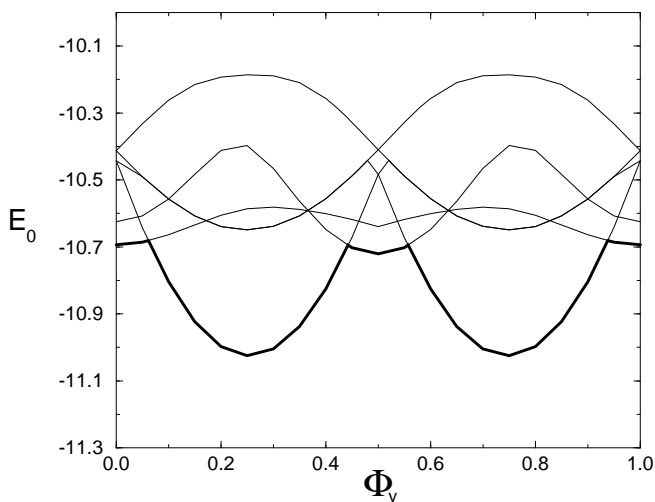


FIG. 8. GS energy vs Φ_y for a 3×8 systems with $V = 2$, $i_0 = 2$, $t_\perp = 0.7$ and closed shell configuration at quarter filling. The thick curve is the absolute GS energy.

A. Charge stiffness: closed shell configuration

In the non-interacting case of a $3 \times L$ system with periodic BC in both directions, t_\perp leads to three branches in k -space separated by an energy of order $\sim t_\perp$ (see Fig. 9). Note that for special values of Φ_y (e.g. $\Phi_y = 0, \frac{1}{2}$), two of them are degenerate. We first consider the closed shell configuration where, for a given momentum k along the chain direction (and sufficiently small t_\perp), the three possible states with different k_\perp momenta ($0, \frac{2\pi}{3}$ or $-\frac{2\pi}{3}$) are either fully occupied or completely empty. In this case, there is a critical value t_\perp^* of t_\perp for which, for an optimum choice of Φ_y , one can move a fermion from one branch to the next with no energy cost. A straightforward calculation gives $t_\perp^* = \sqrt{2/3} \sin(\pi/L)$. Below this value, in the y-direction the bands are filled and therefore no transport can occur in the transverse direction and the Drude weight is vanishing. Note that this quantity t_\perp^* is directly related to the splitting of the bands.

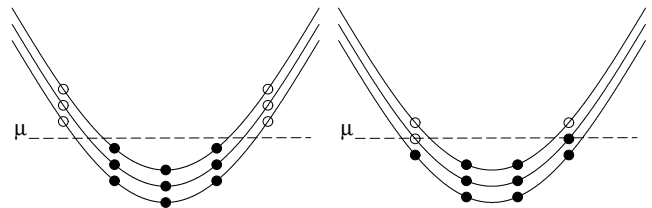


FIG. 9. Dispersion relations as a function of k for closed and open shells.

More generally in the interacting case, the same behaviour is observed as can be seen in Fig. 10 where we plot the Drude weight as a function of t_\perp for a given size. This is a typical behaviour from which one can define some precise cross-over value $t_\perp^*(L)$ where a transition occurs (D_{yy} increases suddenly). Of course, this behaviour is a finite size effect and we must be careful to extract thermodynamic results properly.

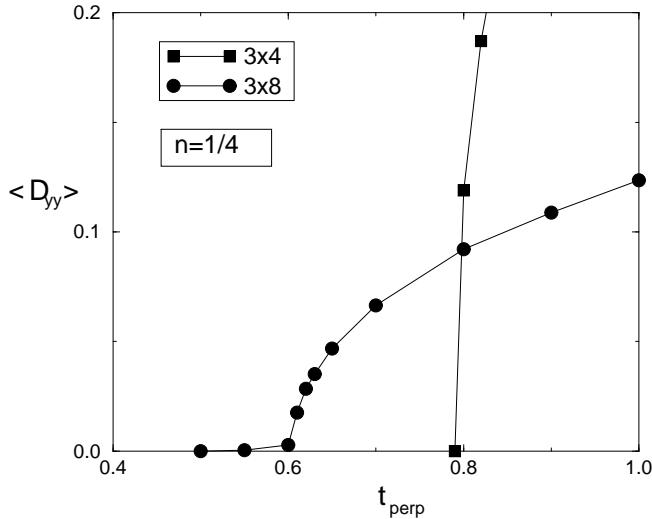


FIG. 10. Drude weight in arbitrary units as a function of t_{\perp} for the case $V = 2, i_0 = 3$ on the 3×4 and 3×8 lattices. An average over Φ_y has been performed according to Eq. (11).

Two scenarios can occur. Firstly, $t_{\perp}^*(\infty)$ might remain finite. In this case, no coherent transport occurs between the chains for sufficiently small t_{\perp} . This is the case, for example, for very strong interactions in the insulating phase. This is also expected in the LL phase for $\alpha > \alpha_0$. Indeed, we expect that $\Delta E = 0$ (see sec. III) would imply $D_{yy} = 0$ (for $L = \infty$). Although it is difficult to prove this behaviour numerically, it is not incompatible with our numerical results. The second possibility is that $t_{\perp}^*(L) \rightarrow 0$ when $L \rightarrow \infty$. In this case, we expect that the non-interacting picture should be approximately valid, at least for not too large an interaction. In other words, according to the non-interacting picture which we discussed above, we expect $t_{\perp}^*(L)$ to be directly related to the splitting ΔE calculated in the previous section.

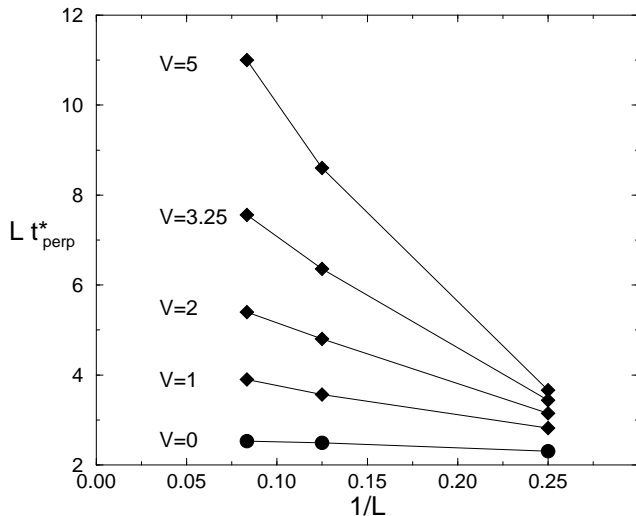


FIG. 11. $L t_{\perp}^*(L)$ as a function of $1/L$ for the non-interacting case (\bullet) and for finite interaction $i_0 = 2$ and $V = 1, 2, 3.25, 5$ (\blacklozenge)

We proceed as follows; we assume a connection between $t_{\perp}^*(L)$ and the splitting ΔE and show that this hypothesis is, indeed, consistent with the numerical data. Let us suppose that $t_{\perp}^*(L)$ fulfills,

$$\max_{\Phi_y} \{ \Delta E(t_{\perp}^*, \Phi_y) \} \sim \frac{2\pi}{L} v_{\rho}, \quad (12)$$

where v_{ρ} is some charge velocity. Thus, $t_{\perp}^*(L)$ should be of order $1/L$, more precisely it should behave like $t_{\perp}^*(L) = A/L + B/L^2$. Finite-size scaling can be performed by plotting $L t_{\perp}^*(L)$ vs $1/L$. As seen in Fig. (11), this scaling law seems to be well satisfied for small interaction strength so that, in this case, a finite-size extrapolation of A is possible. On the other hand, a diverging value of $L t_{\perp}$ (or A) would mean that $t_{\perp}^*(\infty)$ is in fact finite and, hence, completely incoherent hopping occurs. This is likely to occur for the largest values of V we have considered, such as $V = 3.25$ and $V = 5$ and it can not be completely excluded for smaller values of V . According to the qualitative argument of Eq. (12), if $\Delta E(t_{\perp}^*, \Phi_y)$ is linear in t_{\perp} for small t_{\perp} , then $1/A$ is expected to be directly proportional to the extrapolated value of ΔE . In order to check this point, it is convenient to normalize A with respect to the non-interacting case, $A_0 = \sqrt{2/3} \pi$ for $n = 1/4$. The quantity A/A_0 is plotted as a function of the Luttinger parameter α for different values of the interaction in Fig. 12 and compared to the extrapolated value of ΔE obtained for closed shell configurations. Firstly, we remark that, although some error bars are large, the behaviour of t_{\perp}^* seems to be quite similar for different kinds of interactions. In other words, α seems to be the only parameter controlling the behaviour of $1/A$. Secondly, we observe some discrepancies between $1/A$ and ΔE . They can be attributed (i) to the crudeness of the picture we have developed only at a qualitative level, (ii) to the strong dependence of the charge velocity v_{ρ} in Eq. (12) with the interaction and (iii) more importantly, to the fact that the previous estimation of the splitting realized in the closed shell configuration case seems not to be relevant for finite t_{\perp} . Indeed, the second estimation of Sec. III.B of the ratio $\Delta E/2t_{\perp}$, realized for open shell configurations and finite t_{\perp} , gives, for small α , smaller values in better agreement with A_0/A . Moreover, the above extrapolation of $t_{\perp}^*(L)$ assumes $t_{\perp}^*(L = \infty) = 0$, i.e. coherent interchain transport. However, as mentioned above, the possibility of a *small* finite value of $t_{\perp}^*(L = \infty)$ cannot certainly be excluded when $\alpha > 0.2$ which would be in complete agreement with the results for $\Delta E/2t_{\perp}$ obtained in the open shell case.

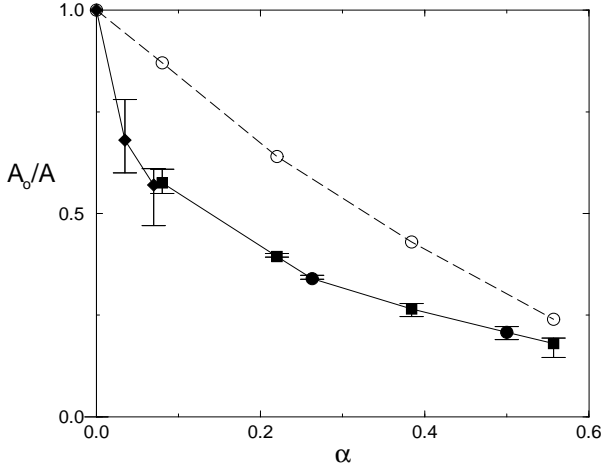


FIG. 12. Extrapolated values of A_0/A as a function of α for different range of interactions $i_0 = 1$ (\blacklozenge), $i_0 = 2$ (\blacksquare) and $i_0 = 3$ (\bullet). For comparison, the extrapolated values of ΔE of Fig. (4) are also reproduced here (open circles).

At this point, we are still left with an incomplete picture. For not too large an interaction ($\alpha < \alpha_0$), our results suggest that D_{yy} is finite for small transverse hopping. Fig. (10) suggests that the slope $\partial\langle D_{yy}\rangle/\partial t_\perp|_{t_\perp=t_\perp^*}$ seems to vanish when $L \rightarrow \infty$. Therefore, a t_\perp^2 behavior of the Drude weight with t_\perp is certainly possible as in the non-interacting case. To have a better understanding of this behaviour we now use a different choice of the boundary conditions along x.

B. Charge stiffness: open shell configuration

By choosing adequate boundary conditions along x ($\Phi_x = 0$ or $\Phi_x = \pi$ depending on the length L), open shells can be realized as seen in Fig. (9). In this case, even for a finite system, the Drude weight and the total kinetic energy remains finite down to vanishing t_\perp as in the non-interacting case. We first consider a fixed value of the flux Φ_y . It is in fact convenient to choose Φ_y corresponding to the lowest GS energy, i.e. such that $\frac{\partial E_0}{\partial \Phi_y} = 0$, since this value (in fact $\Phi_y \sim 0.25$) is almost independent of the interaction and of the system size. The corresponding Drude weight is shown in Fig. 13 for 3×4 , 3×8 and 3×12 systems as a function of t_\perp . Finite size effects are found to be already weak for the two largest cases $L = 8$ and $L = 12$. The Drude weight is clearly strongly suppressed compared to the $V = 0$ case [22].

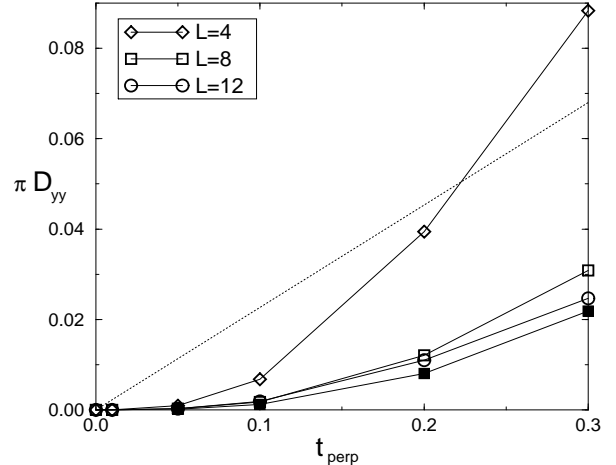


FIG. 13. πD_{yy} for a fixed value of Φ_y (see text), $V = 2$, $i_0 = 3$ and different system sizes $L = 4, 8, 12$ from up to down (open symbols) compared to the averaged data of $L = 8$ (filled squares). The non-interacting case (for a 3×8 torus) is shown as a dotted line.

We now consider an average over Φ_y and we shall denote by $I_{yy} = \langle \int_0^\infty \sigma_{yy}(\omega) d\omega \rangle_{\Phi_y}$ the total sum which is obtained by computing the transverse kinetic energy and averaging over Φ_y . As seen in Fig. 13, the values obtained for the Drude weight by averaging the 3×8 data over Φ_y are very close to the ones obtained on the 3×12 cluster at constant flux. Therefore, it is technically advantageous, as far as CPU time is concerned, to consider smaller systems and perform a flux average. Note that, however, if the number of coupled chains is kept fixed (here $m = 3$), even in the limit $L \rightarrow \infty$, we expect $\langle D_{yy} \rangle_{\Phi_y} \neq D_{yy}(\Phi_y)$ (since the thermodynamic limit is not taken in the direction of the flux). Qualitatively, the averaging procedure mimics many coupled chains. In any case, when confinement within each of the individual chains starts to occur we do not expect crucial differences between the cases of 3 or of an infinite number of coupled chains (if only the t_\perp term couples the chains). In Fig. 14, we plot the Drude weight and the total sum rule as a function of t_\perp for a moderate electronic interaction. We observe that the behavior of these two quantities is not incompatible with the t_\perp^2 law of the non-interacting case [22]. However, the intrachain interaction has drastic effects. Firstly, the total sum rule is strongly reduced compared to $V = 0$ (shown as a reference on Fig. 14). Secondly, it is found that $\pi \langle D_{yy} \rangle_{\Phi_y}$ and I_{yy} behave differently. In other words, for small t_\perp the main fraction of the weight lies in the incoherent part.

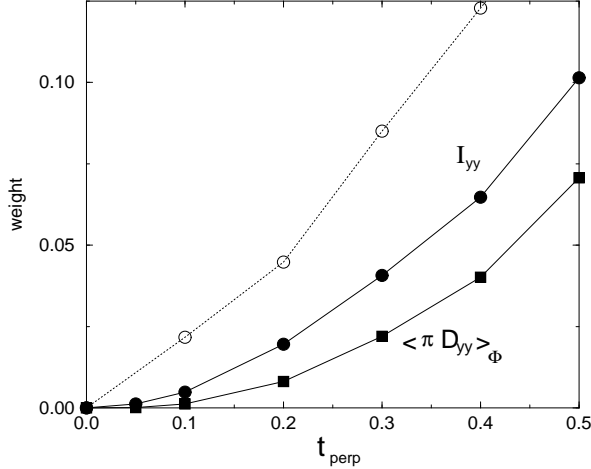


FIG. 14. $\pi\langle D_{yy}\rangle_{\Phi_y}$ (■) and I_{yy} (●) as a function of t_{\perp} for a 3×8 system and $V = 2$, $i_0 = 3$. For comparison, the $V = 0$ case is also displayed as a dotted line.

To be more quantitative, it is convenient to consider the ratio

$$r = \frac{\pi\langle D_{yy}\rangle_{\Phi_y}}{I_{yy}} = \frac{m^2}{4\pi^2} \left\langle \frac{\partial^2 E_0}{\partial \Phi_y^2} \right\rangle_{\Phi_y} / \langle -T_{yy}\rangle_{\Phi_y}, \quad (13)$$

which, as can be seen from the sum rule Eq. (9), corresponds to the relative part of the Drude weight in the total optical conductivity. We have plotted the ratio r for the same 3×8 torus and for the three interaction ranges, $i_0 = 1, 2$ and 3 . The common important feature of these data is that the ratio r decreases as t_{\perp} goes to 0 and can become rather small, typically smaller than 20%. Unfortunately, we think our data become somewhat unreliable for very small t_{\perp} (let's say $t_{\perp} < 0.1$) so that the behavior of the ratio r when $t_{\perp} \rightarrow 0$ cannot be accurately determined. However, our numerical estimates should give the correct trend in the range $0.1 < t_{\perp} < 0.4$.

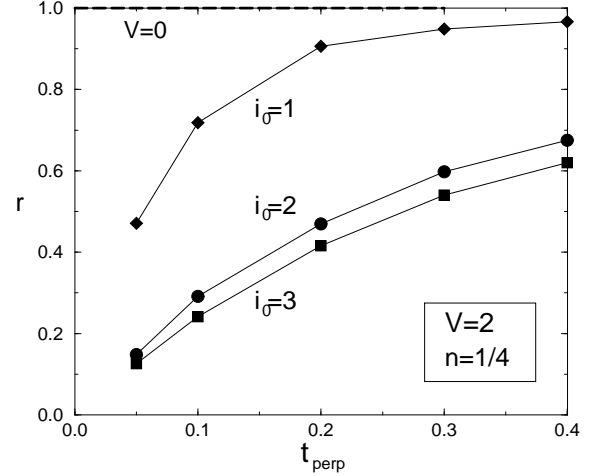


FIG. 15. Ratio of the Drude weight to the total conductivity as a function of t_{\perp} for NN and longer range interaction with the same NN magnitudes $V = 2$.

These results should have very important consequences on the experimental side. Indeed, our results predict, for small t_{\perp} , anomalous transport perpendicular to the chains even when D_{yy} does not completely vanish (if $\alpha < \alpha_0$). Spectral weight is suppressed predominantly from the coherent part of the conductivity. In order to confirm this behaviour, the frequency dependent optical conductivity has been calculated directly and results are discussed in the following.

C. Optical conductivity

The frequency dependence of the transverse optical conductivity can be calculated by use of the Kubo formula,

$$\sigma_{yy}^{reg}(\omega) = \frac{\pi}{N} \sum_{n \neq 0} \frac{|\langle \phi_0 | \hat{j}_y | \phi_n \rangle|^2}{E_n - E_0} \delta(\omega - (E_n - E_0)) \quad (14)$$

where \hat{j}_y is the transverse current operator and the sum runs over all the excited states. So far, we restrict ourselves to the open shell configuration used in the preceding Section. $\sigma_{yy}^{reg}(\omega)$ can be calculated exactly on the same finite clusters by a continued fraction expansion generated by use of the Lanczos method. Firstly, for a given value of Φ_y , one computes the ground state. Here, we choose the absolute GS which carries no current in the y -direction. Then, by applying the transverse current operator on this state, one generates a new vector which serves as the starting point of another Lanczos procedure. Eventually, the tridiagonal form of the hamiltonian in this new basis is used to compute the continued fraction expansion of the regular part of $\sigma_{yy}(\omega)$.

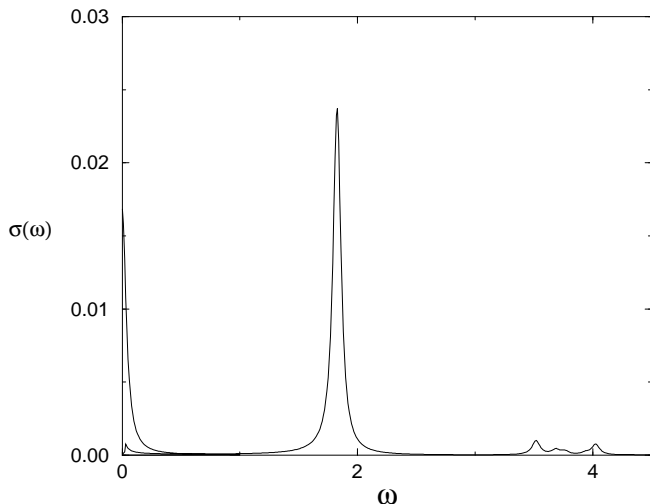


FIG. 16. Transverse optical conductivity vs frequency for a 3×8 system at quarter filling with $V = 2$, $i_0 = 3$ and $t_{\perp} = 0.1$. The Drude δ -function has been represented with the same small imaginary part $\varepsilon = 0.04$.

In the free case, the current operator commutes with the Hamiltonian and therefore, the conductivity only contains a Drude peak. However, as can be seen on Fig. 16, for finite interaction strengths and in the 3×8 cluster, a pronounced structure appears at finite frequency for any small value of t_{\perp} . In order to determine more accurately the position in energy of the weight, we have computed the first moment of the distribution,

$$\langle \omega \rangle = \int_{0+}^{\infty} \sigma_{yy}^{reg}(\omega) \omega d\omega / \int_{0+}^{\infty} \sigma_{yy}^{reg}(\omega) d\omega \quad (15)$$

which is expected to behave smoothly with the various parameters. We observe that it has a finite limit as t_{\perp} goes to 0 (see Fig. 17). This means that, once t_{\perp} is turned on between the chains, weight immediately appears predominantly at finite frequencies. This typical frequency increases with the strength and with the range of the interaction. This is clearly a signature of some form of incoherent perpendicular transport.

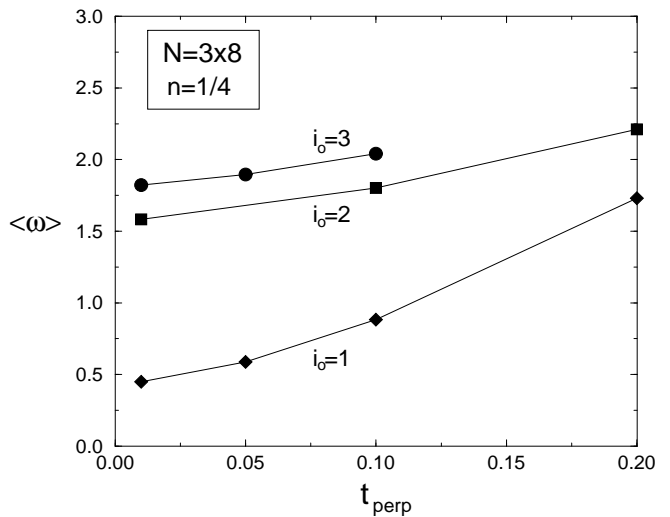


FIG. 17. First moment of the conductivity as a function of t_{\perp} for $V = 2$ and different interaction ranges.

V. CONCLUSIONS

In this work, different approaches to interchain coherence have been investigated. As a first step, we have focussed on the energy splitting generated by the transverse hopping in the dispersion relation of the LL collective modes. By finite size scaling analysis, we have shown that this splitting was monitored by the LL parameter α . However, incoherent interchain hopping is found for much smaller values of α than those predicted by the RG calculations [8]. In the second part of this work, we have attempted to make the connection between the previous energy splitting and transverse transport properties. In the regime where t_{\perp} is still relevant ($\alpha < \alpha_0$), the most important results are that (i) the Drude weight and the total optical sum rule grow less rapidly with t_{\perp} than in the non interacting case and (ii) the Drude weight becomes significantly smaller than the total sum rule when the intrachain interaction is turned on. Hence, even when the Drude weight remains finite (when t_{\perp} is relevant), transverse transport is predominantly incoherent in the small t_{\perp} regime. How small t_{\perp} needs to be so that this regime is observed depends on the strength of the interaction. Typically, for $\alpha \sim 0.2$, strong suppression of coherent transport occurs up to $t_{\perp} \sim 0.15$. This phenomenon could explain the anomalous transport which is observed experimentally.

We gratefully acknowledge many useful discussions and comments from C. Hayward and M. Albrecht. *Laboratoire de Physique Quantique, Toulouse is Unité Mixte de Recherche CNRS No 5626*. We thank IDRIS (Orsay) for allocation of CPU time on the C94 and C98 CRAY supercomputers.

-
- [1] P. W. Anderson, Phys. Rev. Lett. **67**, 3844 (1991); P. W. Anderson, Science **256**, 1526 (1992).
- [2] S. L. Cooper and K. E. Gray in *Physical Properties of High Temperature Superconductors IV*, D. M. Ginsberg (ed.) (World Scientific), 1994; S. L. Cooper et al., Phys. Rev. Lett. **70**, 1533 (1993); Y. Maeno et al., Nature **372**, 532 (1994); X.-D. Xiang et al., Phys. Rev. Lett. **68**, 530 (1992); K. Tamasaku, T. Ito, H. Takagi and S. Uchida, Phys. Rev. Lett. **72**, 3088 (1994).
- [3] C. M. Varma, P. B. Littlewood, S. Schmitt-Rink, E. Abrahams and A. E. Ruckenstein, Phys. Rev. Lett **63**, 1996 (1989).
- [4] F. D. M. Haldane, J. Phys. C **14**, 2585 (1981).
- [5] D. Jérôme and H. Schulz, *Adv. Phys.* **31**, 299 (1982).
- [6] P. Wzietek, F. Creuzet, C. Bourbonnais, D. Jérôme, K. Bechgaard and P. Batail, J. Phys. (Paris) I **3**, 171 (1993).
- [7] K. Behnia et al, Phys. Rev. Lett. **74**, 5272 (1995).
- [8] D. Boies, C. Bourbonnais, and A.-M.S. Tremblay, Phys. Rev. Lett. **74**, 968 (1995).
- [9] D. G. Clarke, S. P. Strong, and P. W. Anderson, Phys. Rev. Lett. **72**, 3218 (1994).
- [10] D. G. Clarke and S. P. Strong, cond-mat/9607141 preprint.
- [11] F. Mila and D. Poilblanc, Phys. Rev. Lett. **76**, 287 (1996).
- [12] M. Fabrizio & A. Parola, Phys. Rev. Lett. **70**, 226 (1993).
- [13] C. Lanczos, J. Res. Natl. Bur. Stand. **45**, 255 (1950).
- [14] D. Poilblanc, H. Endres, F. Mila, M. Zacher, S. Capponi and W. Hanke, Phys. Rev. B (in press) and cond-mat/9605106 preprint.
- [15] W. Kohn, Phys. Rev. **133**, A 171 (1964).
- [16] D. Poilblanc, Phys. Rev. B **44**, 9562 (1991).
- [17] C. Gros, Z. Phys. B **86**, 359 (1992).
- [18] J. Voit, Rep. Prog. Phys. **58**, 977 (1995) and references therein.
- [19] J. Voit, Phys. Rev. B **47**, 6740 (1993).
- [20] H. J. Schulz, “*Correlated Electron Systems*”, p. 199, ed. V. J. Emery (World scientific, Singapore, 1993); H. J. Schulz, “*Strongly Correlated Electronic Materials: The Los Alamos Symposium – 1993*”, p. 187, ed. K. S. Bedell, Z. Wang, D. E. Meltzer, A. V. Balatsky, E. Abrahams (Addison-Wesley, Reading, Massachusetts, 1994).
- [21] P. Maldague, Phys. Rev. B **16**, 2437 (1977).
- [22] For a finite system of non-interacting fermions, the $D_{yy}(t_{\perp})$ curve is made of linear segments the slope of which increases with t_{\perp} . The t_{\perp}^2 -law is recovered in the thermodynamic limit when the average length of the segments vanishes. This peculiar behavior makes finite size scaling analysis of the transverse conductivity at finite V difficult.